

Strongly interacting fermions

K. F. Quader

Department of Physics, University of Illinois at Urbana-Champaign, 1110 West Green Street, Urbana, Illinois 61801

K. S. Bedell

T11, Mail Stop B262, Los Alamos National Laboratory, Los Alamos, New Mexico 87545

G. E. Brown

Department of Physics, State University of New York at Stony Brook, Stony Brook, New York 11794

(Received 1 December 1986)

It is shown that strongly interacting Fermi systems, such as ^3He , transition metals, and the heavy-fermion systems can be consistently described within the "induced"-interaction Fermi-liquid formalism. The general limiting features of the model are considered. In agreement with the Gutzwiller (half-filled case) solution to the Hubbard model, there is a localization of excitations as $F_0^{\uparrow} \rightarrow \infty$ and $F_1^{\uparrow} \rightarrow \infty$. Some of the large m^* originate from a large "dynamic" mass, m_λ for f electrons, which is then shown to be further increased by many-body effects. In disagreement with the Gutzwiller solution in the half-filled case, but in agreement with the less-than-half-filled case, the compression modulus goes to a finite value as $F_0^{\uparrow}, F_1^{\uparrow} \rightarrow \infty$, so that—in a jellium model—the Debye frequency Θ_D has a finite value. The implication of the spin-dependent parameter F_0^{\uparrow} going to a finite limit are discussed. In particular, it is shown that ferromagnetic ordering cannot occur in the case of a short-ranged potential.

I. INTRODUCTION

Strongly interacting fermions appear in a variety of systems which may have interesting relations with each other. Examples of these are liquid ^3He , some of the Laves-phase metals, such as UAl_2 and TiBe_2 , and the heavy-fermion (or heavy-electron) systems such as UPt_3 , UBe_{13} , U_6Fe , URu_2Si_2 , CeCu_2Si_2 , etc.

The heavy-fermion systems are an exciting class of materials that have been of great current interest. (For a review of the experimental properties, see Refs. 1 and 2, and for the theory, see Refs. 3 and 4.) At high temperature the heavy-fermion systems behave like a collection of independent magnetic ions. Though not quite clear how, as the temperature is lowered, a coherence sets in between the localized f electrons; this gives rise to the low-temperature Fermi-liquid behavior which is a characteristic of the heavy-electron metals. The Fermi liquid that develops has several outstanding features. The first, of course, is the large coefficient of the linear term in the specific heat, $\gamma = C_v/T$, which is 10^2 – 10^3 times larger than in the simple metals. Another is that the susceptibility χ is very large and proportional to γ . Also, the temperature dependence of the resistivity for small T can be fit by an expression, $\rho(T) = \rho_0 + \alpha T^2$. In the clean heavy-fermion metals, $\alpha \sim 1/T_F^2 > 0$, T_F being the Fermi temperature of the heavy electrons. The different ground states that one encounters in these systems are *superconducting* as in UPt_3 , UBe_{13} , U_6Fe , URu_2Si_2 , and CeCu_2Si_2 , *antiferromagnetic* as in U_2Zn_{17} , UCd_{11} , and URu_2Si_2 , and *normal* as in CeAl_3 and CeCu_6 . Though it is not clear why one ground state is favored over another, there seems to exist some correlation between χ and γ .

In this paper, we shall discuss the calculation of the

Fermi-liquid interaction parameters in strongly interacting Fermi systems. Thus, we shall assume the existence of a well-defined Fermi liquid at low temperatures.

Fermi-liquid theory, as developed by Landau, was a phenomenological theory, in which the Fermi-liquid parameters were obtained from experiment. It has proved, in fact, very difficult to calculate the large Fermi-liquid parameters in, for example, liquid ^3He from microscopic models. In nuclear physics, however, the interactions are substantially weaker, the Fermi-liquid parameters being of order unity, and considerable progress has been made in formulating a quantitative microscopic Fermi liquid theory. Some of this work is summarized in Bäckman *et al.*⁵ Completely microscopic theories have not enjoyed much success in deriving Fermi-liquid parameters for liquid ^3He . An approach based on the Babu-Brown *induced-interaction model*⁶ was introduced by Ainsworth, Bedell, Brown, and Quader (hereafter referred to as ABBQ).⁷ This compromise between microscopic and phenomenological approaches has met with considerable success. The induced-interaction model has since been generalized to treat two-component systems such as spin-polarized liquid ^3He ,⁸ extended to include momentum-dependent interactions,⁹ and applied to different Fermi systems.¹⁰

Here, we shall concentrate on the general aspects as well as the limiting features of the induced-interaction model. We shall discuss how in a broad sense, this general framework can be applied to encompass different and sometimes interrelated strongly interacting Fermi systems. In so doing, we shall discuss the work of ABBQ on transition metals, and elaborate on the work of Bedell and Quader,¹¹ who showed that this formalism could give a description of the heavy-fermion systems.

The model system under consideration is a two-level itinerant one with parabolic dispersion for the excitation energy spectrum. In the case of spin- $\frac{1}{2}$ liquid ^3He and spin-symmetric nuclear matter, this is quite apt; in the heavy-fermion systems the assumption is that the crystal fields lift the degeneracy of the f level to give a Kramers doublet in the ground state. These can then be viewed as effective spin- $\frac{1}{2}$ Fermi systems with spherical Fermi surfaces. Though the description effectively is that of a one-band Fermi liquid, some of the essential features such as hybridization with other bands and their effects on the quasiparticles under study are incorporated into the underlying Hamiltonian. Isotropy is assumed, however, Galilean invariance is not invoked, hence the invariance-breaking band masses, etc., can be treated within the scheme.

The organization of the paper is as follows. In Sec. II, we outline the relationship of the effective mass m^* to the Landau interaction parameters for Fermi liquids without Galilean invariance. A general discussion of the full effective mass m^* , the "dynamic" mass m_λ , and the various contributions to them including the energy-dependent ones, is given in Sec. III. Section IV is devoted to a general discussion of the induced-interaction model and the developments leading up to the formulation of the "direct" or driving terms in some explicit cases. The general solutions, including the illustrative schematic ones, for large strengths of the driving interactions are discussed in Sec. V. The limiting features of the model are also discussed in detail there. A comparison of this approach to others in the large enhancement limit is given in Sec. VI. We remark on the electron-phonon interactions in metals in Sec. VII, and on pairing in the context of the induced-interaction model in Sec. VIII. We end with a summary and concluding remarks in Sec. IX.

II. FERMILIQUID THEORY FOR SYSTEMS WITHOUT GALILEAN INVARIANCE

Most of the previous solutions of Fermi-liquid theory with the induced-interaction model referred to Galilean-invariant systems. The connection between the effective mass m^* and the $l=1$ Fermi-liquid parameter F_1^s for a system that is not translationally invariant has been discussed by Pines and Nozières¹² and by Leggett.¹³ We outline this for an isotropic Fermi surface. The total current \mathbf{J} is given by

$$\mathbf{J} = \sum_{\mathbf{p}, \sigma} (\nabla \varepsilon_{\mathbf{p}\sigma}) n_{\mathbf{p}\sigma}, \quad (2.1)$$

where $\varepsilon_{\mathbf{p}\sigma}$ is the quasiparticle energy and $n_{\mathbf{p}\sigma}$ is the distribution function. Near the Fermi surface one has

$$\begin{aligned} \mathbf{J} &= \sum_{\mathbf{p}, \sigma} \mathbf{v}_{\mathbf{p}\sigma} \left[\delta n_{\mathbf{p}\sigma} - \frac{\partial n_{\mathbf{p}}^{(0)}}{\partial \varepsilon_{\mathbf{p}}} \sum_{\mathbf{p}', \sigma'} f_{\mathbf{p}\mathbf{p}'}^s \delta n_{\mathbf{p}'\sigma'} \right] \\ &= \sum_{\mathbf{p}, \sigma} \mathbf{j}_{\mathbf{p}\sigma} \delta n_{\mathbf{p}\sigma}. \end{aligned} \quad (2.2)$$

Here $|\mathbf{v}_{\mathbf{p}\sigma}| = |(\partial \varepsilon_{\mathbf{p}\sigma} / \partial \mathbf{p})_{k_F}| = k_F / m^*$ and $\mathbf{j}_{\mathbf{p}\sigma}$ is the quasiparticle current. If the quasiparticle interaction $f_{\mathbf{p}\mathbf{p}'}^s$

is expanded in a Legendre series in the Landau angle, $\cos \theta_L = \hat{\mathbf{p}} \cdot \hat{\mathbf{p}}'$, we have,

$$f_{\mathbf{p}\mathbf{p}'}^s = \sum_l f_l^s P_l(\cos \theta_L). \quad (2.3)$$

If this is used in Eq. (2.2) then for $p = k_F$,

$$j_{k_F} = v_F (1 + F_1^s / 3), \quad (2.4)$$

where $F_1^s = (k_F m^* / \pi^2) f_1^s$, f_1^s being the $l=1$ term in Eq. (2.3) and $m^* k_F / \pi^2$ is the density of states at the Fermi surface. Since for *non-Galilean-invariant* systems, the current is no longer carried by the bare mass m on defining $j_{k_F} = k_F / m_\lambda$ we get

$$\frac{m^*}{m_\lambda} = 1 + F_1^s / 3. \quad (2.5)$$

After rearranging we find

$$\frac{m^*}{m} = \frac{m_\lambda / m}{1 - \frac{1}{3} \bar{F}_1^s}, \quad (2.6)$$

where

$$\bar{F}_1^s = \frac{k_F m_\lambda}{\pi^2} f_1^s. \quad (2.7)$$

The quantity m_λ , in principle, has contributions coming from band structure, phonons, etc., and has been referred to as the dynamic mass.¹³ If the band mass is already quite large, one can see that quite modest f_1^s 's can lead one to very large m^* 's. The limiting behavior should be noted: $m^* \rightarrow \infty$ as $\bar{F}_1^s \rightarrow 3$. This may thus introduce another mass into the problem for systems without Galilean invariance.

III. EFFECTIVE MASSES m^* AND m_λ

Since the dynamic mass m_λ can enter into the problem in certain cases, it is worthwhile dwelling on it for a bit. It is not clear how to calculate a m_λ for a particular system, though it is possible to extract it from experiments.¹³ A physical interpretation could be given as follows. When a quasiparticle moves through the medium, it displaces other quasiparticles. The interactions give rise to a contribution to the effective mass due to the backflow of the displaced quasiparticles. The size of this effect is given by F_1^s . Thus m_λ is the mass the quasiparticle would have in the absence of backflow. We expect m_λ / m to be large compared with unity for narrow- f -band metals. Thus, before the additional Fermi-liquid effects, one already has a large mass enhancement $m_\lambda / m \sim 0(10)$.

The dynamic mass m_λ as defined in Ref. 13, can be measured in experiments in which the normal quasiparticle current vanishes. In the superconducting phase it is possible to obtain this from the temperature dependence of the penetration depth in the London limit.¹³ At $T=0$ the London penetration depth is given by¹³

$$\lambda^{-2}(T=0) = \frac{4\pi n e^2}{m_\lambda c^2}, \quad (3.1)$$

where n is the total number density, and c is the speed of light.

In principle it is possible to measure m_λ (or F_1^s) if an absolute measurement can be made. The recent experiments of Einzel *et al.*¹⁴ could only measure the change in $\lambda(T)$ at low T . Nevertheless, they were able to place a bound on F_1^s in UBe₁₃, i.e., $F_1^s < 20$. There are many sources of finite temperature corrections to $\lambda(T)$ in UBe₁₃ which makes the value of F_1^s somewhat uncertain. But it does seem clear that F_1^s by itself cannot explain the large value of m^*/m , and is possibly not large.

In a calculation of m_λ for the narrow- f -band systems, the band mass coming from the static lattice should be a sizeable contributor to this mass. There are additional contributions to this coming from phonons and the Coulomb interaction. The Coulomb contributions are distinct from the Fermi-liquid effects coming from F_1^s . This can be seen in the formulation of the Fermi-liquid theory for a charged system. In the charged system the Coulomb term, $4\pi e^2/q^2$, is explicitly removed from the quasiparticle interaction.¹² Thus, when calculating the dynamic mass m_λ the contributions from this term must be included.

It is, unfortunately, not possible to naively replace m_λ with the effective mass calculated using the standard techniques, e.g., local-density-functional methods. The reason is that, although screened potentials giving many-body effects are used, approximations are made which drop the energy dependence (ω dependence) of the electron-electron interactions. These provide appreciable mass enhancements.

Said briefly, the effective mass at the Fermi surface is given by

$$\frac{m^*}{m} = \frac{1 - \left. \frac{\partial \Sigma(\mathbf{p}, \omega)}{\partial \omega} \right|_{\omega=E_F}}{1 + \left. \frac{\partial \Sigma(\mathbf{p}, \omega)}{\partial T_p} \right|_{\omega=E_F}}, \quad (3.2)$$

where the numerator can be connected with Z_p , the weighting at the quasiparticle pole

$$Z_{p_F} = \frac{1}{1 - \left. \frac{\partial \Sigma(\mathbf{p}, \omega)}{\partial \omega} \right|_{\omega=E_F}}. \quad (3.3)$$

Band-structure calculations include, through hybridization, the mixing of f electrons with the other electrons. But the wave function in a band calculation is essentially a Slater determinant, and does not contain components such as an excited f electron or conduction electron plus collective excitation. Just the coupling to such components, which involves not only matrix elements but also energy denominators, brings in a strong ω dependence and enhances the numerator in Eq. (3.2).

Let us restate the situation in other words. The density-functional calculations give us a representation consisting of a set of single-particle orbitals much as a Hartree-Fock calculation would do. These contain the band mass. Coupling to more complicated configurations, such as orbitals above the Fermi surface plus collective excitations, is not included in the density-functional calculation and must be put in through Fermi liquid theory.

These latter couplings produce the ω -dependent contributions to the effective mass—the numerator of (3.2)—and the related renormalization at the quasiparticle pole, Eq. (3.3).

A somewhat analogous situation has been treated in nuclear physics.¹⁵ Thomas-Fermi, Hartree-Fock, or Brueckner-Hartree-Fock calculations there provide a representation and produce the “ k mass,” the denominator of (3.2). Dynamic effects, which produce the “ ω mass” must be put in by Fermi-liquid theory. Reference 15 relates this situation to that in liquid ³He and electrons in metals.

Finally, we mention that it has been suggested¹⁶ that in the heavy-fermion systems the effective mass m^* could be related to the $l=0$ Landau parameters, F_0^s ,

$$\frac{m^*}{m} = 1 + F_0^s, \quad (3.4)$$

where $F_0^s = (k_F m^* / \pi^2) f_0^s$. Thus, the effective mass,

$$\frac{m^*}{m} = \frac{1}{1 - (k_F m / \pi^2) f_0^s}, \quad (3.5)$$

would diverge if $(k_F m / \pi^2) f_0^s \rightarrow 1$.

IV. INDUCED INTERACTION MODEL

A. General discussion

We wish to describe a simple, soluble Fermi-liquid theory for strongly interacting systems, starting from a microscopic description, albeit with some empirical input. It has been known^{6,8} that a consistent Fermi-liquid theory cannot be formulated in terms of *short-range effective interactions* alone; *collective excitations* generated by these must be exchanged between the quasiparticles. Functional differentiation of the two types of self-energy, shown in Fig. 1, and further generalizations^{6,8} lead to integral equations (see Fig. 2) for the Fermi-liquid interactions on the Fermi surface $f_{pp'}^{\sigma\sigma'}$.

The main point is that the contributions to $f_{pp'}^{\sigma\sigma'}$ can be separated into two parts:^{6,8}

$$f_{pp'}^{\sigma\sigma'} = d_{pp'}^{\sigma\sigma'} + I_{pp'}^{\sigma\sigma'} [f_{pp'}^{\sigma\sigma'}], \quad (4.1)$$

where the *induced* part, $I_{pp'}^{\sigma\sigma'}$, a function of the Landau interactions $f_{pp'}^{\sigma\sigma'}$ themselves, is particle-hole reducible in the

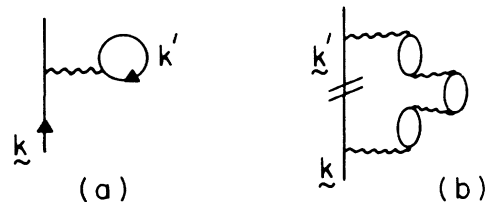


FIG. 1. The two types of contribution to the quasiparticle self-energy: (a) the Hartree-Fock interaction involving a short-range pseudopotential; (b) the self-energy arising from emission and absorption of a collective excitation. The interaction making up the collective excitation is here shown to be the same as in (a), but later it will be taken to be the full Fermi-liquid interaction $f_{\mathbf{k}\mathbf{k}'}^{\sigma\sigma'}$. The undertildes denote 4-vectors.

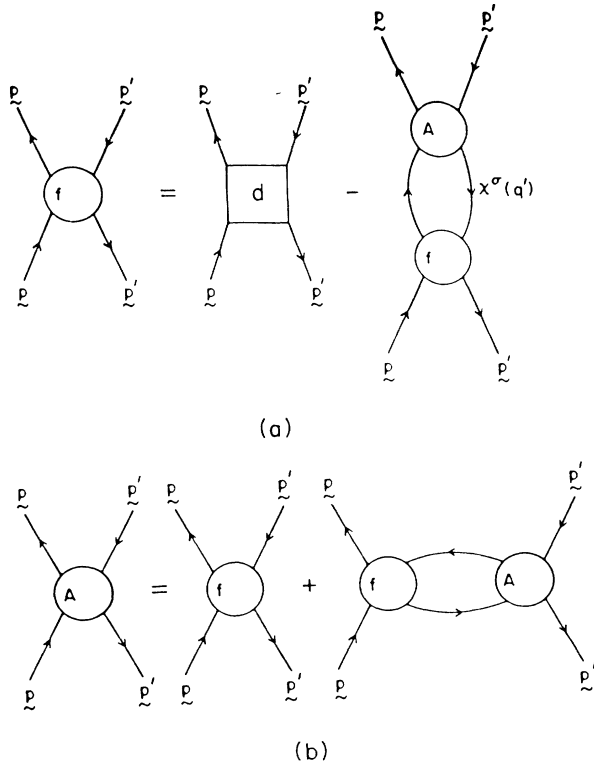


FIG. 2. Graphical representation of the “induced” interaction model integral equations: (a) for the Landau interaction $f_{pp'}^{\sigma\sigma'}$; (b) for the scattering amplitudes $a_{pp'}^{\sigma\sigma'}$.

exchange particle hole, i.e., u channel, whereas the *direct* part, $d_{pp'}^{\sigma\sigma'}$ is not particle-hole reducible in either the direct particle hole, i.e., t channel or the crossed channel, i.e., u channel. In physical terms, $I_{pp'}^{\sigma\sigma'}$ includes the contributions from the exchange of virtual collective excitations, for example, density, spin-density, current, or spin-current fluctuations between the quasiparticles.

Another way to understand the induced interactions is to note that $I_{pp'}^{\sigma\sigma'}$ arise naturally from the fully reducible four-point vertex functions on demanding that the scattering amplitudes, $a_{pp'}^{\sigma\sigma'}$ on the Fermi surface are properly antisymmetrized.⁸ As shown in Fig. 2(b), $a_{pp'}^{\sigma\sigma'}$ contains the contributions from the direct particle-hole channel. Once an appropriately antisymmetrized direct interaction, $d_{pp'}^{\sigma\sigma'}$ is chosen, the set of equations in Fig. 2 will guarantee that the Landau forward-scattering sum rule is satisfied. Since $I_{pp'}^{\sigma\sigma'}$ contains the exchange or u -channel contributions, the set of equations in Fig. 2, especially with the momentum dependence treated more generally,⁹ are *crossing symmetric* in the two particle-hole channels. Moreover, vertex corrections⁸ have been taken into account in a way that the initial and final vertices (in addition to the intermediate ones) in $I_{pp'}^{\sigma\sigma'}$ (u channel) are the Landau $f_{pp'}^{\sigma\sigma'}$ themselves. Thus, by construction, adequate conserving approximations have been built into the set of equations. A discussion of the induced-interaction model in the light of the more microscopic “parquet” approach can be found in Ref. 17.

For a single-component (or one-band) Fermi system, the interaction,

$$f_{pp'}^{\sigma\sigma'} = f_{pp'}^s + f_{pp'}^a \cdot \sigma \cdot \sigma', \quad (4.2)$$

where $f_{pp'}^s$ and $f_{pp'}^a$ are the symmetric (s) and antisymmetric (a) spin combinations. Then the induced-interaction equations are as follows:

$$F_{pp'}^s = D_{pp'}^s + \frac{1}{2} \frac{F_0^s U_0(q') F_0^s}{1 + F_0^s U_0(q')} + \frac{3}{2} \frac{F_0^a U_0(q') F_0^a}{1 + F_0^a U_0(q')} + \frac{1}{2} \left[1 - \frac{q'^2}{4k_F^2} \right] \left[\frac{F_1^s U_1(q') F_1^s}{1 + F_1^s U_1(q')} + 3 \frac{F_1^a U_1(q') F_1^a}{1 + F_1^a U_1(q')} \right], \quad (4.3)$$

$$F_{pp'}^a = D_{pp'}^a + \frac{1}{2} \frac{F_0^s U_0(q') F_0^s}{1 + F_0^s U_0(q')} - \frac{1}{2} \frac{F_0^a U_0(q') F_0^a}{1 + F_0^a U_0(q')} + \frac{1}{2} \left[1 - \frac{q'^2}{4k_F^2} \right] \left[\frac{F_1^s U_1(q') F_1^s}{1 + F_1^s U_1(q')} - \frac{F_1^a U_1(q') F_1^a}{1 + F_1^a U_1(q')} \right], \quad (4.4)$$

where the quantities in Eqs. (4.3) and (4.4) have been multiplied by the interacting density of states $N(0) = m^* k_F / \pi^2$ to make them dimensionless. The momentum transfer in the crossed particle-hole channel, $q'^2 = |\mathbf{p} - \mathbf{p}'|^2 = k_F^2 (1 - \cos \theta_L)$, with the Landau angle $\theta_L = \hat{\mathbf{p}} \cdot \hat{\mathbf{p}}'$, and $N(0)U_0(q')$ and $N(0)U_1(q')$ are the Lindhard functions or density-density and current-current correlation functions, respectively. These are given in the Appendix.

The first term in Eqs. (4.1), (4.3), and (4.4) for $f_{pp'}^{\sigma\sigma'}$, the so-called *direct interaction*, is somewhat of a misnomer since the direct interaction being antisymmetrized contains both the direct and exchange scattering terms. The term is designed to convey the fact that the two quasiparticles can directly scatter via some effective potential, and repeatedly so, as in the G matrix. The direct term is of short range and contains information about the underlying Hamiltonian of the system under consideration. Thus, it is the driving term. The induced term is of somewhat longer range since two particles can scatter via an interaction mediated by another particle. Since the induced terms are a function of the exchange particle-hole channel momentum, q' , they can contribute to all the moments, $f_i^{s,a}$ [Eq. (2.4)] even for zero range $D^{s,a}$. These are obtained by Legendre projections.

B. Development

In some sense, certain energy scales are expected to underly the strongly interacting systems. To some extent, the characterization of our direct interactions in the physical systems is roughly based on such energy scales. For example, in the case of transition metals or the heavy-fermion systems for which the Anderson Hamiltonian or the finite-range Hubbard model may be appropriate starting points, the scales could be the following.

(i) Strong on-site electron-electron interaction, $O(10^4 - 10^5 \text{ K})$ in the heavy-fermion case.

- (ii) Nearest-neighbor interaction, down by an order of magnitude $O(10^3-10^4 \text{ K})$.
- (iii) Degeneracy or Fermi energy $O(10^2 \text{ K})$.
- (iv) Energy of the low-lying collective excitation, for example, spin-fluctuation energy $O(10 \text{ K})$.

It may be noted that within the context of the Kondo model, one encounters an energy scale, the Kondo temperature associated with Kondo resonance in the system.

A hierarchy similar to (i)–(iv) also exists in liquid ^3He . For example, at melting pressure, one obtains the same ordering by dividing the numbers in (i)–(iv) by 10^2 .

The direct interaction has a spin dependence similar to $f_{pp'}^{\sigma\sigma'}$:

$$D_{pp'}^{\sigma\sigma'} = D_{pp'}^s + D_{pp'}^a \cdot \sigma \cdot \sigma' . \quad (4.5)$$

Often these are expanded in Legendre polynomials, $D_{pp'}^{s,a} = \sum_{l=0} D_l^{s,a} P_l(\cos\theta_L)$, and a few of the moments are retained. A purely zero-range interaction U , like in the usual Hubbard model,¹⁸ would imply $D_0^s = -D_0^a = U/2$. For ^3He , finite-range corrections are important; ABBQ treated D_0^s , D_0^a , and D_1^s phenomenologically so as to reproduce the empirical F_0^s , F_0^a , and F_1^s and predicted F_1^a and the higher ($l \geq 1$) $F_l^{s,a}$'s. For the transition metals, the nearest-neighbor, i.e., finite-range corrections arise from the direct overlap of wave functions. These have been estimated¹⁸ to be an order of magnitude down from the on-site interaction U . Accordingly, the $l=1$ direct interaction were included by ABBQ to describe transition metals.

In the case of heavy-fermion systems, the distance of separation between the f -atom sites is large, and direct overlaps are probably small.¹⁹ However, finite-range interactions could be induced via the coupling of the heavy electrons to those in the conduction band, similar to the Ruderman-Kittel-Kasuya-Yosida type interactions. Thus, Bedell and Quader¹¹ modeled the direct part of the interaction by a *finite-ranged renormalized* potential:

$$D_0^{\dagger\dagger} = \left[1 - \frac{\alpha}{2} \right] U , \quad (4.6)$$

$$D_0^{\dagger\uparrow} = -\frac{\alpha U}{2} .$$

With $D_l^{\sigma\sigma'} (l \geq 2) = 0$, this on antisymmetrization gives

$$D_0^s = (1 - \alpha) \frac{U}{2} ,$$

$$D_0^a = -\frac{U}{2} , \quad (4.7)$$

$$D_1^s = D_1^a = \frac{\alpha U}{4} .$$

$D_0^{\dagger\dagger}$ represents the strong intra-atomic repulsion between particles with opposite spins; $D_0^{\dagger\uparrow}$ is the nearest-neighbor corrections to U with $\alpha \sim O(\frac{1}{10})$. Having $D_1^s = D_1^a$ in Eqs. (4.7) is tantamount to having a *local* potential; this has been done for simplicity. As will be discussed later, a *nonlocal* potential would give unequal D_1^s and D_1^a , as well as generate $l > 1$ direct terms.

We shall study in detail the consequences of using Eqs.

(4.6)–(4.7) in the direct part of the induced-interaction model; in particular, as U is varied. The main results will not depend on the precise choice of the value of α ; but they will depend on its sign. Here $\alpha > 0$, $\alpha = 0$ being a special case.

That $\alpha > 0$ can be understood qualitatively as follows. As an example, consider the f -electron systems. Let v_{fc} be the interaction between the f and conduction electrons. This will induce an interaction between the f electrons. To second order in v_{fc} the interaction between parallel-spin f electrons would be of the form

$$d_{pp'}^{\dagger\dagger} = v_{fc}^2 [-N_c(0)U_0(q=0) + N_c(0)U_0(q')] , \quad (4.8)$$

where $q'^2 = |\mathbf{p} - \mathbf{p}'|^2 = 2k_F^2(1 - \cos\theta)$. This form satisfies the constraint that $d_{pp'}^{\dagger\dagger}$ is antisymmetrized since under exchange, \mathbf{q} and \mathbf{q}' are interchanged. The factor $-N_c(0)U_0(q) [-N_c(0)U_0(q')]$ is the lowest-order direct (exchange) particle-hole propagator (Lindhard function) for the conduction band. For small q' ;

$$U_0(q') \simeq 1 - \frac{1}{12} \left[\frac{q'}{k_F} \right]^2 + \dots .$$

If we use this in Eq. (4.8) we find,

$$d_{pp'}^{\dagger\dagger} \simeq \frac{1}{12} v_{fc}^2 N_c(0) \left[\frac{q'}{k_F} \right]^2$$

$$= -\frac{1}{6} v_{fc}^2 N_c(0) (1 - \cos\theta) . \quad (4.9)$$

From this we have that

$$d_0^{\dagger\dagger} = d_0^s + d_0^a = -\frac{1}{6} v_{fc}^2 N_c(0) \quad (4.10)$$

and

$$d_1^{\dagger\dagger} = d_1^s + d_1^a = \frac{1}{6} v_{fc}^2 N_c(0) > 0 . \quad (4.11)$$

A full two-band calculation would yield a more complicated dependence on v_{fc} and U for $d_{pp'}^{\dagger\dagger}$, however, the sign of $d_1^{\dagger\dagger}$ would not change. Thus, we see that a finite-range term in the direct interaction could be generated by a coupling induced between the f electrons via the conduction electrons.

V. SOLUTIONS AND RESULTS

For strongly interacting systems, we are interested in the complete self-consistent solution of the coupled integral equations, Eqs. (4.3) and (4.4) for large values of U . In this context, the limiting model behavior for $U \rightarrow \infty$ will prove to be interesting. Before we consider the exact solutions, let us discuss them *schematically*. This should give insight into the salient features of the model.

To leading order, in Eqs. (4.3) and (4.4),

$$\frac{F_0^s U_0(q') F_0^s}{1 + F_0^s U_0(q')} \rightarrow F_0^s \quad (5.1)$$

and terms on the right-hand side of Eq. (4.3) involving F_1^s and F_1^a can be neglected. Thus, to this order, $D_0^s \sim U/2$ and $F_0^s \cong U$. As a result of delicate cancellations, the solution for F_0^a is more subtle and one has to be more careful in trying to obtain the correct value for it. We

shall return to this later. It is, however, clear from inspection of Eq. (4.4) that F_0^a will decouple from the direct interaction and from the density modes. Since D_0^a equals $-U/2$, and the second term on the right-hand side of Eq. (4.4) is approximately $+U/2$, we can see that these two individually large terms cancel each other to a very good approximation. We are left, then, with only the induced interaction pieces involving F_0^a and the velocity-velocity interactions on the right-hand side of Eq. (4.4). In this lowest order, which amounts to setting $\alpha=0$, $F_0^a \approx -\frac{2}{3}$ as found by ABBQ.

In the next order, we keep only terms of order αU , which will involve only terms linear²⁰ in $\cos\theta_L$, since we are not interested in corrections of order α to F_0^s and F_0^a . These equations are

$$\delta F_{pp'}^s \cong \frac{\alpha U}{4} \cos\theta_L + \frac{1}{4} \cos\theta_L \frac{F_1^s U_1(q') F_1^s}{1 + F_1^s U_1(q')} + \frac{3}{4} \cos\theta_L \frac{F_1^a U_1(q', 0) F_1^a}{1 + F_1^a U_1(q')}, \quad (5.2)$$

$$\delta F_{pp'}^a = \frac{\alpha U}{4} \cos\theta_L + \frac{1}{4} \cos\theta_L \frac{F_1^s U_1(q') F_1^s}{1 + F_1^s U_1(q')} - \frac{1}{4} \cos\theta_L \frac{F_1^a U_1(q') F_1^a}{1 + F_1^a U_1(q')}, \quad (5.3)$$

where $\delta F_{pp'}^{s,a} \cong F_{pp'}^{s,a} - F_0^{s,a}$. Since our scheme involves considering αU to be large compared with unity, these give a value of F_0^a more negative than $-\frac{2}{3}$, and

$$F_1^s = \frac{\alpha U}{4} + \frac{1}{4} F_1^s + \frac{3}{4} F_1^a, \quad (5.4)$$

$$F_1^a = \frac{\alpha U}{4} + \frac{1}{4} F_1^s - \frac{1}{4} F_1^a, \quad (5.5)$$

giving

$$F_1^s = \frac{2}{3} \alpha U, \quad (5.6)$$

$$F_1^a = \frac{1}{3} \alpha U, \quad (5.7)$$

in conformity with the full self-consistent calculation of Bedell and Quader.¹¹

In discussing the complete solution to Eqs. (4.3) and (4.4), it should be noted that for large U these equations simplify somewhat. The resulting forms given in the Appendix [Eqs. (A7)–(A10)], give the resulting equations for

$F_0^{s,a}$ and $F_1^{s,a}$. These can now be solved for the $F_l^{s,a}$'s. As discussed earlier, α has been fixed at $\alpha=0.1$, and for a particular effective mass in the density of states, the model can be solved for any value of U . For *Galilean invariant* systems, the effective mass is the total or the thermal mass, m^*/m which is related to F_1^s (Secs. II and III). Since for the *non-Galilean-invariant* case, m^*/m is related to F_1^s only through the dynamic mass m_λ (Secs. II and III) it is then useful to use the density of states $\bar{N}(0) \equiv m_\lambda k_F / \pi^2$. This however, requires knowing the ratio m^*/m_λ in addition to the thermal mass m^* .

In Table I we reproduce from Ref. 11. the Landau parameters $F_0^{s,a}, F_1^{s,a}$ as a function of U , and the corresponding quantities, denoted by an overbar, with $\bar{N}(0)$ as the density of states. We have also calculated the higher order Landau parameters. To show that these are not negligible, we present these $F_l^{s,a}$'s ($l \leq 5$) in Table II.

The general limiting features of the model is evident.

(a) For a *finite* α , as $U \rightarrow \infty$, with $N(0)$ as the density of states,

$$\begin{aligned} F_0^s &\rightarrow U, \\ F_1^s &\rightarrow \frac{2}{3} \alpha U, \\ F_1^a &\rightarrow \frac{1}{3} \alpha U, \\ F_0^a &\rightarrow \text{const.} (\approx -0.906), \end{aligned} \quad (5.8)$$

in conformity without our schematic solutions. It is seen that F_0^s and $F_1^{s,a}$ diverge as m^*/m_λ diverges, while $F_0^a \rightarrow \text{const.}$, independent of α or m_λ .

For the same α , but for the quantities with $\bar{N}(0)$, one gets

$$\begin{aligned} \bar{U} &\rightarrow \bar{U}_{\text{crit}} = \frac{9}{2\alpha}, \\ \bar{F}_0^s &\rightarrow \left[1 - \frac{\alpha}{6} \right] \bar{U}_{\text{crit}}, \\ \bar{F}_1^s &\rightarrow \frac{2}{3} \alpha \bar{U}_{\text{crit}} = 3, \\ \bar{F}_1^a &\rightarrow \frac{1}{3} \alpha \bar{U}_{\text{crit}}, \end{aligned} \quad (5.9)$$

and

$$\bar{F}_0^a \rightarrow 0.$$

(b) If $\alpha \rightarrow 0$, i.e., for a purely *contact* direct interaction,

TABLE I. The Bedell-Quader (Ref. 11) calculated values of the Fermi-liquid parameters, $F_l^{s,a}$ ($l=0,1$) and m^*/m_λ for different large values of U ; the density of states is $N(0) = m^* k_F / \pi^2$. $\bar{F}_l^{s,a}$ and \bar{U} 's have been obtained by dividing $F_l^{s,a}$ and U by m^*/m_λ and hence have density of states $\bar{N}(0) = m_\lambda k_F / \pi^2$

U	\bar{U}	F_0^s	\bar{F}_0^s	F_0^a	\bar{F}_0^a	F_1^s	\bar{F}_1^s	F_1^a	\bar{F}_1^a	m^*/m_λ
150	30.11	-0.879	-0.176	149	29.95	4.3	0.87	12	2.4	5
1000	41.61	-0.900	-0.037	985	40.97	32.7	1.36	69	2.87	24
4500	44.14	-0.904	-0.009	4426	43.42	149.3	1.46	302	2.97	102
9000	44.60	-0.905	-0.004	8851	43.86	299.4	1.48	602	2.98	202
25 000	44.85	-0.905	-0.002	24585	44.10	832.7	1.49	1669	2.99	557
10^8	44.99	-0.906	-4×10^{-7}	9.8×10^7	44.25 ^a	3.3×10^7	1.5 ^a	6.7×10^3	3.00 ^a	2.2×10^6

^aRounded off to the second decimal place.

TABLE II. The calculated higher order ($l > 1$) Landau parameters corresponding to different choices of $U = N(0)u$ (see Table I) and m^*/m_λ . The corresponding quantities with overbars can be obtained from these on dividing by m^*/m_λ .

U	m^*/m_λ	F_2^a	F_2^s	F_3^a	F_3^s	F_4^a	F_4^s	F_5^a	F_5^s
150	5	-0.46	1.43	-0.15	0.47	-0.06	0.14	-0.01	0.06
1000	24	-0.68	2.24	-0.23	0.66	-0.10	0.30	-0.03	0.09
4500	102	-0.74	2.44	-0.25	0.71	-0.11	0.35	-0.03	0.10
25 000	557	-0.75	2.49	-0.26	0.72	-0.12	0.36	-0.03	0.10

$$\begin{aligned} \bar{U}_{\text{crit}} &\rightarrow \infty, \\ \bar{F}_0^s &\rightarrow \infty, \\ \bar{F}_0^a &\rightarrow 0 (F_0^a \rightarrow -\frac{2}{3}), \end{aligned} \quad (5.10)$$

while m^*/m remains finite. This has been considered in some detail by ABBQ. In the Gutzwiller solution²¹ to the Hubbard model with only a contact interaction, $F_0^a \rightarrow -\frac{3}{4}$.

We point out that the resulting behavior of F_1^a above, is a consequence of the choice of a *local* direct interaction. This choice was made for simplicity. Inclusion of a *non-local* piece would change F_1^a . For example, in the ABBQ calculation for ^3He , a negative F_1^a is obtained.

In case (a), i.e., for a nonzero, positive α , the model then has immediate implications.

The susceptibility χ diverges owing to m^*/m_λ diverging. In other words, the quantity

$$\frac{\chi}{\mu_{\text{eff}}^2 N(0)} = \frac{1}{1 + F_0^a} \quad (5.11)$$

remains finite independent of the value of U , μ_{eff} being the effective magnetic moment of the fermion. Then, since the mass diverges without the onset of ferromagnetic ordering, this is equivalent to the *metal-insulator transition* of the Mott type.²²

In the induced-interaction model, the suppression of ferromagnetic ordering is a consequence of the feedback mechanism inherent in Eqs. (4.3) and (4.4). The onset of a ferromagnetic phase transition is signaled by a divergence in the scattering amplitude A_0^a where

$$A_0^a = \frac{F_0^a}{1 + F_0^a} \rightarrow -\infty. \quad (5.12)$$

This scattering amplitude must be fed back into the equation for f_{pp}^a , which comes via the induced term. In general, F_0^a will depend only weakly on the direct interaction. For the choice, Eqs. (4.6) and (4.7), as we push $U \rightarrow +\infty$, together the equation for f_{pp}^a decouples from the potential as outlined above and assumes a value independent of U . The detailed derivation is given in Eqs. (A12)–(A16) in the Appendix. Thus, looking for a ferromagnetic instability by simply looking at the divergence in a single channel, i.e., A_0^a would miss this feedback effect.

As an example, it may be noted that liquid ^3He in this model looks much more like a Gutzwiller solid, which we shall discuss later, than as if it were close to going ferromagnetic, since F_0^a is not so close to -1 . If the system were close to going ferromagnetic, all the $F_l^a/2l + 1$ would be large. Here, in fact, is one of the significant features of the model; namely, if one includes the correla-

tions in both particle-hole channels to all orders, then a system with a short-ranged potential will not go ferromagnetic no matter how strong the potential.

This does not mean that a Fermi liquid cannot go ferromagnetic. It simply means that it cannot get there with a short, though, finite-ranged potential. Clearly, we are building in a certain amount of physics by introducing a short-ranged potential for the direct scattering between the quasiparticles. It is plausible that a systematic inclusion of the higher-order moments in the direct and induced interaction will push one closer to the ferromagnetic instability. However, one has to bear in mind the inherent feedback mechanism of the model. Thus, as one gets closer to the ferromagnetic instability, the direct interaction will also have higher-order partial waves. The reason is that it contains, among other things, the exchange of two or more spin fluctuations in the particle-particle channel. As these become “soft,” it will produce more structure in the direct interaction thereby generating higher order partial waves. At this point it is not possible to be more precise about the nature of the ferromagnetic transition within the context of the model.

In the above sense, our model is different from that of Rice and Ueda,²³ who evaluated the periodic Anderson model with a Gutzwiller approximation. Rice and Ueda find that the heavy-fermion liquid is stable against magnetic order only in rather special cases.

VI. COMPARISON WITH OTHER MODELS

It will be of interest to understand the connection and difference between our model, the usual Gutzwiller models^{21,22} and the recent ones of Rice and Ueda.²³ Velocity dependence enters in a more explicit way in our model, driven by the D_1^a and the D_1^s . In the Gutzwiller model, the numerator of Eq. (3.2) is obtained from Z_{p_f} , Eq. (3.3). These are just differences of form. The chief difference of physics is in the importance in our model of the exchange Coulomb interaction, which produces the large F_0^a . The Coulomb interaction is probably also responsible for the input velocity dependence. Considerable study^{21–24} has been given to the Gutzwiller variational solution to the Hubbard model as the interaction strength U become large, and this has been used²⁵ as a model for heavy-fermion systems. Gutzwiller²⁶ introduces a simple Jastrow-type correlation to partially empty out doubly occupied sites, arriving at a simple expression for the ground-state energy per lattice point

$$\epsilon = Z^1 \epsilon_1 + Z^1 \epsilon_1 + Ud. \quad (6.1)$$

Here Z^σ is the discontinuity at the Fermi surface; d is the

probability of a site being doubly occupied. As U approaches a critical value U_c , $Z^\sigma \rightarrow 0$ and $d \rightarrow 0$. For this U_c , every lattice point is singly occupied; i.e., the particles are localized.

More explicitly, in the neighborhood of U_c ,

$$\frac{m^*}{m} \cong \frac{1}{1 - (U/U_c)^2}. \quad (6.2)$$

From (3.2) and (3.3) one sees that $Z^\sigma \rightarrow 0$ as $U \rightarrow U_c$, where $U_c = 8|\epsilon_0|$ and $\epsilon_1 = \epsilon_i = \epsilon_0$ in zero field. From the general relation that Z^σ represents the discontinuity in occupation number n_k at the Fermi surface, we see that n_k is continuous here in the limit $m^* \rightarrow \infty$. This is what would be expected from localization of the quasiparticles, a complete localization in space implying a complete spread in quasiparticle momenta.

Obviously, perturbation theory wouldn't work in this situation, because as $Z \rightarrow 0$, there are no quasiparticles left. This is reminiscent of the Skyrme model for the nucleon²⁷ which can be achieved²⁸ in the chiral bag model by letting the bag radius $\rightarrow 0$. In this limit, the quarks (quasiparticles) disappear, the origin becoming a nucleation point, and the nucleon becomes all meson cloud. Quantum numbers are, however, preserved. We believe the situation to be similar with the induced interaction equations. Enough general requirements, in particular, the Landau sum rule, are built in so that they seem to remain sensible in the limit $Z^\sigma \rightarrow 0$.

There are important differences between the Gutzwiller solution and our Fermi-liquid result. Firstly, the Hubbard model to which the Gutzwiller solution applies, treats fermions on a lattice. Depending upon the particular type of lattice one obtains an antiferromagnetic state for a value of U less than U_c . Liquid ^3He is a liquid, and it is not clear why this model should give a reasonable description; one does not expect magnetic ordering in the liquid. Although there may be tendencies towards antiferromagnetic ordering in the systems we discuss, these do not seem to be important for the main features.

In this discussion, the behavior of F_0^s which diverges as $(m^*/m)^2$ as $U \rightarrow U_c$ in the usual Gutzwiller model^{21,22} (exactly half-filled band) is relevant. This means that the compression modulus κ , which goes as F_0^s/m^* for large m^* , goes to ∞ as $U \rightarrow U_c$. In our model κ remains finite as $m^* \rightarrow \infty$. In a jellium model, as we will show in Sec. VII, where the motions of the lattice and electrons are simply tied together, the Debye frequency Θ_D goes as $[(m^*/m_\lambda)/(1+F_0^s)]^{1/2}$. In the Gutzwiller model, $\Theta_D \rightarrow \infty$, as $U \rightarrow U_c$, indicating that the electrons localize on a static incompressible lattice. From the results of the induced interaction model Θ_D is finite in the large m^* limit. This is consistent with the heavy-fermion systems where the Θ_D 's are not very large; they are several hundred degrees Kelvin. It should be noted that in the recent Gutzwiller model of Rice and Ueda²³ where the bands are not exactly half-filled, $F_0^s \propto m^*/m$ as in our model.

Another important difference between the Gutzwiller solution to the Hubbard Hamiltonian and our model is F_1^q . In the Gutzwiller approach, the effective mass m^* is obtained by relating it to the discontinuity at the Fermi surface, $Z^{-1} \propto m^*$. From Eq. (2.5) it is then possible to

extract F_1^s . However, there is no equivalent procedure for obtaining F_1^q within this approach. It has been obtained for example by Vollhardt²¹ by using the forward scattering sum rule, this gives $F_1^q \approx -0.75$ when $U \rightarrow U_c$. In contrast, the induced interaction model calculates F_1^q and all of the higher-order Landau parameters. In fact, we find that $F_1^q \rightarrow \frac{1}{2}F_1^s$ as $m^* \rightarrow \infty$, although this depends on our assumption that $D_1^s = D_1^q$ as discussed earlier. These values may change if, for example, we include the momentum dependence of the Landau parameters or a *nonlocal* term in the direct interaction. As argued by Bedell and Quader¹¹ there is no *a priori* reason to believe that F_1^q will remain finite when $U \rightarrow U_c$, i.e., $m^* \rightarrow \infty$. This depends on how close F_0^s is to -1 . The closer F_0^s gets to -1 , the larger F_1^q and the other partial waves must become to satisfy the sum rule.

VII. ELECTRON-PHONON INTERACTIONS IN METALS

We shall discuss the case where the phonon-induced interaction will be considerably modified due to the many-body correlations. In the context of the jellium model for the phonons we can obtain explicit expressions for the sound velocity, S_{ph} , as well as the phonon-mediated interaction between the electrons. From the former we can define the Debye frequency, $\Theta_D = k_D S_{\text{ph}}$, where $k_D = (3/Z)^{1/3} k_F$. From the latter we should be able to study the role the phonons will play in the superconducting transition. We should emphasize from the outset that there is no reason to expect the jellium model to be applicable to the heavy-fermion systems: As we will see, however, it does provide a reasonable estimate for the Debye frequency in these systems.

To calculate S_{ph} we must first determine the renormalized phonon frequency ω_q , where¹²

$$\omega_q^2 = \Omega_{\text{pl}}^2 - \frac{q^2}{4\pi e^2} |v_q^i|^2 \left[1 - \frac{1}{\epsilon(q,0)} \right]. \quad (7.1)$$

The ion plasma frequency is given by

$$\Omega_{\text{pl}}^2 = \frac{4\pi n_i (Ze)^2}{M},$$

where n_i is the density, M the mass, and Z the valence, of the ion. The bare electron-ion coupling is given by

$$|v_q^i|^2 = \frac{(4\pi Ze^2)^2 n_i}{q^2 M}. \quad (7.2)$$

The dielectric function for the electrons, $\epsilon(q, \omega)$, includes the Fermi-liquid corrections and the dynamic-mass effects. In the limit $\omega = 0$ this takes on the simple form,¹²

$$\epsilon(q, 0) = 1 + \frac{\omega_{\text{pl}}^2}{S^2 q^2} \quad (7.3)$$

with $\omega_{\text{pl}}^2 = 4\pi n_e e^2 / m_\lambda$ and $m_\lambda S^2 = \frac{2}{3} \epsilon_F (1 + F_0^s)$. Note that m_λ and not the optical mass,¹³ m_{opt} , appear in Eq. (7.3). The reason is that m_{opt} appears in high-frequency conductivity, whereas Eq. (7.3) is evaluated at $\omega = 0$. If the band mass is large in the heavy-fermion systems, then m_{opt} will also be quite large. This would result in a plas-

ma frequency that is small compared with simple metals. A measurement of the plasma frequency could in principle give us some insight into the size of the band mass.

If we now plug Eqs. (7.2) and (7.3) into Eq. (7.10) we find, that

$$\omega_q^2 = S_{\text{ph}}^2 q^2,$$

where

$$S_{\text{ph}}^2 = \left[\frac{m_\lambda}{M} Z \right] S^2. \quad (7.4)$$

This result, Eq. (7.4), differs from the usual jellium result for simple metals in several important ways. The first is the fact the m_λ and not m appears in Eq. (7.4). Additionally, the Fermi-liquid corrections are included in the usual way.¹² In the simple metals these effects are not very large, however, in the heavy-fermion systems they are crucial. We can write Eq. (7.4) as

$$S_{\text{ph}}^2 = \frac{Z}{3M} \frac{k_F^2}{m} \left[\frac{1 + F_0^s}{m^*/m} \right]. \quad (7.5)$$

It is clear that $\Theta_D = S_{\text{ph}} k_D$ will, as previously noted, diverge in the usual Gutzwiller^{21,22} model while it approaches a finite value in the induced interaction approach.

We can make some simple estimates for the Debye frequency of UPt₃ and UBe₁₃. Assuming that $m_\lambda/m = 10$, we find $\Theta_D = 277$ K for UPt₃ and $\Theta_D = 440$ K for UBe₁₃. Here we have taken the ionic mass to be that of the uranium ion with a valence of $Z = 3$. The experimental values of Θ_D are 210 and 620 K for UPt₃ and UBe₁₃, respectively. If we naively apply this to the U₆X (Mn, Fe, Co, Ni) compounds we get a $\Theta_D \sim 500$ K, where the experimental value is 100 K.²⁹ Although this difference is large in the U₆X compounds, we believe that this is most likely due to the simple assumption that only one of the uranium atoms is involved in the vibration. If we assume that all six uraniums vibrate together we get a $\Theta_D \simeq 250$ K, the precise value depending rather weakly on Z .

To obtain the phonon induced interaction we must first take into account two modifications of the bare electron-ion interaction, v_q^i . The first is the screening of this interaction due to the presence of the other electrons, $v_q^i/\epsilon(q, 0)$.¹² The other correction comes when we take into account the Fermi-liquid corrections to the electron ion vertex. If we put this all together we have,

$$v_q^{\text{eff}} = \frac{v_q^i}{(1 + F_0^s)\epsilon(q, 0)}. \quad (7.6)$$

We define now the phonon induced interaction,

$$V(q, \omega) = |v_q^{\text{eff}}|^2 \frac{1}{\omega^2 - \omega_q^2}. \quad (7.7)$$

In the limit $\omega \rightarrow 0$ we obtain

$$N(0)V(q, 0) = -\frac{1}{(1 + F_0^s)}. \quad (7.8)$$

In the absence of other mechanisms it is this interaction that would determine the superconducting transition. But, as we will see, there are other interactions that will compete with this in the heavy-fermion systems.

From either the induced interaction model or the Gutzwiller model we see that the phonon induced interaction is strongly screened since $F_0^s \gg 1$. That this interaction $V(q, 0)$ should be screened can be understood rather simply. The phonon induced interaction is basically a deformation potential. As such, the electrons interact via this potential by producing a fluctuation in the ion density. However, since the electrons in a jellium model are tied to the ions, the density of the electrons will also be deformed. To do this we must overcome the incompressibility of the electrons which brings in the screening factor, $(1 + F_0^s)$. This screening will have an important consequence in the superconducting transition in the heavy-fermion systems, and should not be ignored in models that have phonon mediated pairing.³⁰

VIII. SUPERCONDUCTIVITY

It has been suggested that the superconductivity in the heavy-fermion compounds is caused by Fermi-liquid effects^{11,25,31,32} which favor formation of spin-1 pairs, analogous to the situation in liquid ³He. For the heavy fermion, as in liquid ³He, the spin fluctuations should favor triplet pairing. An electron going through the material polarizes the electrons it passes so that their spins tend to be parallel with its spin. A second electron, passing through with its spin in the same direction, benefits from this polarization. Of course, this requires that the Fermi-liquid interaction is attractive in spin-1 states.

To determine the pairing we make use of the Patton-Zaringhalam approximation.³³ For now we will ignore the phonon contribution to pairing. We only remark that the phonons will tend to favor singlet and suppress triplet pairing. In this approximation we have

$$T_c = 1.13 T^* e^{1/g_1}, \quad (8.1)$$

where $T^* = \alpha T_F$ and $\alpha \ll 1$. The pairing amplitude g_1 for triplet pairing is given by

$$g_1 = \frac{1}{12} (A_0^s + A_0^a - A_1^s - A_1^a), \quad (8.2)$$

where $A_l^{s,a} = F_l^{s,a}/(1 + F_l^{s,a}/2l + 1)$. Two approximations are involved here. The first is the s - p approximation. Truncating at $l = 1$ waves, the Landau amplitude is taken from 0° to 180° by reversing the sign of the $l = 1$ amplitudes. Since the sum of the four A 's is zero, by the Landau sum rule, we can write

$$g_1 = \frac{1}{6} (A_0^s + A_0^a) \quad (8.3)$$

which may be more directly useful, because $A_0^s = 1$ for large F_0^s . At least in the case of UPt₃, A_0^a can be obtained directly from the $T^3 \ln T$ term in the specific heat.³² One need not stick with the s - p approximation, nor need one truncate the series in A_l at $l = 1$. The induced-interaction equations are designed for calculating the large-angle scattering, truncation in l being made only in the driving

terms D_l . The idea is (as explained in ABBQ), that the direct terms describe the short-range interaction, for which this truncation should be justified, whereas the F_l 's coming from the long-range phonon-exchange interaction included in the induced interaction, will not converge as rapidly. It has been shown⁹ that in the case of liquid ^3He such a solution of the induced interaction equations represents a great improvement over the s - p approximation for the viscosity and spin-diffusion coefficient, which involve the large-angle scattering.

The basic approximation in the Patton-Zarlingham approach is the incorrect inclusion of the phase space from $E=0$ to αT_F in the A_l 's; this should be excluded because the A_l 's are later to be used in this "model space" to compute the pairing. The lowest energy scale entering into the A_l 's is the spin-fluctuation energy

$$E_{\text{SF}} \approx (1 + F_0^a) E_F. \quad (8.4)$$

The incorrect inclusion of the model space of dimension αT_F in the interaction to be used later for the pairing calculation leads to errors of order $\alpha T_F / E_{\text{SF}}$. Now αT_F is a cutoff, analogous to the Debye cutoff in BCS theory, which reflects the fact that the interactions we consider (spin fluctuations) are highly frequency dependent, and the expression used for the effective interaction is valid only for a restricted range of energies T^* in the immediate vicinity of the Fermi surface. Choosing the cutoff so as to obtain the correct value of T_c at zero pressure, one finds³³ $\alpha = 0.01$. Thus, $\alpha T_F / E_{\text{SF}} \approx \frac{1}{20}$ and the Patton-Zarlingham approach should be good. A detailed discussion of the superconductivity in UPt_3 is given in Ref. 32. Inclusion of Fermi-liquid parameters for higher l , i.e., $F_l^{a,s}$ for $l \geq 2$ (see Table II) would decrease T_c by only $\sim 5\%$.

It is more significant here that g_1 will saturate. Thus, for values of $m^*/m_\lambda > 5$, g_1 will not change very much. The transition temperature should then scale with T^* which in turn varies inversely with m^* . This agrees to a good approximation with the T_c trend as we go from UPt_3 (UBe_{13} and CeCu_2Si_2), to U_2PtC_2 , to U_6Fe . This increasing of T_c with decreasing mass will not continue. At some point the phonon mechanism will begin to turn on since F_0^s is decreasing with decreasing m^* , thereby, reducing the screening of $V(q,0)$. As the phonon mediated interaction becomes more important it will tend to favor the singlet pairing and suppress the triplet. The pairing interaction will then be affected causing a rapid decrease in T_c . This, Bedell and Quader¹¹ argued, is why systems such as Pd and TiBe_2 may not go superconducting. In these systems there are strong spin-fluctuation effects as well as strong phonon effects. They will tend to cancel each other out thereby pushing T_c to very low temperatures or suppressing superconductivity altogether. This led Bedell and Quader¹¹ to speculate that there should be a class of systems with effective masses smaller than U_6Fe but larger than TiBe_2 that are superconducting but with a transition temperature less than that in U_6Fe . Subsequent experiments by DeLong *et al.*²⁹ on $\text{U}_6 X$ ($X = \text{Mn, Fe, Co, Ni}$) have shown a trend consistent with these speculations.

IX. CONCLUSION

In this paper, we have shown that the induced interaction model can be used to describe strongly interacting Fermi systems. One of the important qualitative features of this model is that it can account for systems with a wide variation in energy scales. These large variations in energy scales are typical of such systems as ^3He and the heavy-electron metals. As a result, Bedell and Quader¹¹ had applied this model to the heavy-fermion systems. Here, we have provided further details, and extensions of that work. Additionally, we have tried to give a comprehensive discussion of the various features of the model in general, with allusion to other strongly interacting systems.

An important feature to be emphasized is the onset of localization, and the suppression of long-range ferromagnetic ordering in the large U [$=N(0)u$] limit. As we have shown, in this model for a short-range effective potential, localization sets in before the onset of ferromagnetism.

A virtue to the induced interaction approach is that with a small number of parameters, it enables one to calculate consistently the static, as well as, transport properties of interacting Fermi systems for $T \ll T_F$. Thus, starting with a coherent Fermi liquid as the ground state, a wide variety of excitation properties of such systems can be described adequately. The induced interaction calculations in various systems,^{7,8,10} and the subsequent extension to finite momentum transfers^{9,34} have provided very good accounts of the thermodynamic, transport, and pairing properties of unpolarized and spin-polarized ^3He . Our discussions here, and those in Ref. 11, show that though quite suggestive, it is not possible at present to make as detailed a comparison between theory and experiment for the heavy-electron systems. Calculations that take into consideration more than one band, and hybridization between them are under study.

ACKNOWLEDGMENTS

We would like to thank Phil Allen, Sudip Chakravarty, Steve Koonin, Tony Leggett, Chris Pethick, and David Pines for useful and informative discussions. This work was supported in part by the National Science Foundation under Grant No. DMR 82-15128 and in part by the U.S. Department of Energy under Contract No. DE-AC02-76 ER12001.

APPENDIX A

In Sec. V we discuss the schematic solutions of Eqs. (4.3) and (4.4). This contains the essential features of the complete self-consistent solution model which we outline in this appendix. First we can write Eqs. (4.3) and (4.4) as

$$F_{\text{pp}'}^s = D_{\text{pp}'}^s + \frac{1}{2}[\gamma^s(q') + 3\gamma^a(q')] + \frac{1}{4}[\beta^s(q') + 3\beta^a(q')], \quad (A1)$$

$$F_{\text{pp}'}^a = D_{\text{pp}'}^a + \frac{1}{2}[\gamma^s(q') - \gamma^a(q')] + \frac{1}{4}[\beta^s(q') - \beta^a(q')], \quad (A2)$$

where

$$\gamma^{s,a}(q') = \frac{(F_0^{s,a})^2 U_0(q')}{1 + F_0^{s,a} U_0(q')}$$

and

$$\beta^{s,a}(q') = (1+x) \frac{(F_1^{s,a})^2 U_1(q')}{1 + F_1^{s,a} U_1(q')}, \quad (\text{A3})$$

with $q'^2 = 2k_F^2(1-x)$; $x = \cos\theta_L$. The functions $U_0(q')$ and $U_1(q')$ are given by

$$U_0(q') = \frac{1}{2} \left[1 + \left[\frac{q'}{4k_F} \right] \ln \left| \frac{k_F - q'/2}{k_F + q'/2} \right| \right] \quad (\text{A4})$$

$$U_1(q') = \frac{1}{2} \left[\frac{3}{8} - \frac{k_F^2}{2q'^2} + \left[\frac{k_F^3}{2q'^3} + \frac{k_F}{4q'} - \frac{3q'}{32k_F} \right] \times \ln \left| \frac{k_F - q/2}{k_F + q'/2} \right| \right].$$

In the large- U limit we have,

$$\gamma^s(q') \equiv F_0^s \left[1 - \frac{1}{F_0^s U_0(q')} \right] \quad (\text{A5})$$

and

$$\beta^s(q') \equiv F_1^s (1+x) \left[1 - \frac{1}{F_1^s U_1(q')} \right].$$

We now substitute Eqs. (A5) into Eqs. (A1) and (A2) to obtain the moments $F_l^{s,a}$ where,

$$F_l^{s,a} = \frac{2l+1}{2} \int_{-1}^1 dx F_{pp}^{s,a} P_l(x). \quad (\text{A6})$$

For $F_0^{s,a}$ and $F_1^{s,a}$ we then have,

$$F_0^s = D_0^s + \frac{1}{2} F_0^s + \frac{1}{4} F_1^s + \frac{1}{4} (2c_0 + d_0) + \frac{3}{2} \gamma_0^s + \frac{3}{4} \beta_0^s, \quad (\text{A7})$$

$$F_1^s = D_1^s + \frac{1}{4} F_1^s - \frac{1}{4} (2c_1 + d_1) + \frac{3}{2} \gamma_1^s + \frac{3}{4} \beta_1^s, \quad (\text{A8})$$

$$F_0^a = D_0^a + \frac{1}{2} F_0^a + \frac{1}{4} F_1^s - \frac{1}{4} (2c_0 + d_0) - \frac{1}{2} \gamma_0^a - \frac{1}{4} \beta_0^a, \quad (\text{A9})$$

$$F_1^a = D_1^a + \frac{1}{4} F_1^s - \frac{1}{4} (2c_1 + d_1) - \frac{1}{2} \gamma_1^a - \frac{1}{4} \beta_1^a, \quad (\text{A10})$$

where

$$\gamma_l^a = \frac{2l+1}{2} \int_{-1}^1 dx P_l(x) \gamma^a(q'),$$

$$\beta_l^a = \frac{2l+1}{2} \int_{-1}^1 dx P_l(x) \beta^a(q'),$$

and

$$c_l = \frac{2l+1}{2} \int_{-1}^1 dx \frac{P_l(x)}{U_0(q')},$$

$$d_l = \frac{2l+1}{2} \int_{-1}^1 dx \frac{(1+x)}{U_1(q')} P_l(x).$$

(A11)

In the large enhancement limit, F_0^a will, in general, depend only weakly on the direct interaction, and for the choice of the direct interaction given by Eqs. (4.6) and (4.7), it will decouple from the direct interaction. To see how this comes about we eliminate F_0^s and F_1^s from the right side of Eqs. (A6)–(A10). Thus

$$F_0^s = 2D_0^s + \frac{2}{3} D_1^s + 3\gamma_0^s + \gamma_1^s + \frac{1}{3} (3\beta_0^s + \beta_1^s) - \frac{1}{2} (2c_0 + d_0) - \frac{1}{6} (2c_1 + d_1), \quad (\text{A12})$$

$$F_1^s = \frac{4}{3} D_1^s + 2\gamma_1^s + \beta_1^s - \frac{1}{3} (2c_1 + d_1), \quad (\text{A13})$$

$$F_0^a = - (D_1^a + \frac{1}{3} D_1^s) + \gamma_0^a + \gamma_1^a + \frac{1}{2} (\beta_0^a + \beta_1^a) - \frac{1}{2} (2c_0 + d_0) - \frac{1}{6} (2c_1 + d_1), \quad (\text{A14})$$

and

$$F_1^a = D_1^a + \frac{1}{3} D_1^s - \frac{1}{3} (2c_1 + d_1). \quad (\text{A15})$$

Now in the *local* potential model [i.e., with Eqs. (4.6) and (4.7)], in the limiting case, $F_1^a \rightarrow \infty$ and F_0^a becomes

$$F_0^a = (D_0^s + D_0^a + D_1^s + D_1^a) + \gamma_0^a + \gamma_1^a - (c_0 + d_0 + c_1 + d_1) = \gamma_0^a + \gamma_1^a - (c_0 + d_0 + c_1 + d_1), \quad (\text{A16})$$

where we have used $\sum_{l=0}^1 D_l^s + D_l^a = 0$.

We can see from Eq. (A14) that in general F_0^a is decoupled from the $l=0$ moment of the direct interaction; however, it will depend on the $l=1$ and higher-order moments. Note however that F_1^a could be made negative by the proper choice, for example with a *nonlocal* potential even though F_1^s would still be very large. This in turn would make F_0^a smaller in magnitude. The features have been explored to some extent in ABBQ.

¹G. R. Steward, Rev. Mod. Phys. **56**, 755 (1984).

²Z. Fisk, H. R. Ott, T. M. Rice, and J. L. Smith, Nature **320**, 124 (1986).

³P. A. Lee, T. M. Rice, J. W. Serene, L. J. Sham, and J. W. Wilkins, Comments Cond. Mat. Phys. **12**, 99 (1986).

⁴C. J. Pethick and D. Pines (unpublished).

⁵S.-O. Bäckman, G. E. Brown, and J. Niskanen, Phys. Rep. **124**, 1 (1985).

⁶S. Babu and G. E. Brown, Ann. Phys. **78**, 1 (1973).

⁷T. L. Ainsworth, K. S. Bedell, G. E. Brown, and K. F. Quader,

J. Low Temp. Phys. **50**, 315 (1983).

⁸K. F. Quader and K. S. Bedell, J. Low Temp. Phys. **58**, 89 (1985); K. S. Bedell and K. F. Quader, Phys. Lett. **96A**, 91 (1983); Phys. Rev. B **30**, 2894 (1984).

⁹T. L. Ainsworth, in *Condensed Matter Theories*, edited by F. B. Malik (Plenum, New York, 1986), Vol. 1, p. 129; T. L. Ainsworth and K. S. Bedell, Phys. Rev. B **35**, 8425 (1987).

¹⁰K. F. Quader and K. S. Bedell, Phys. Rev. B **31**, 1627 (1985); K. S. Bedell and D. E. Meltzer, Phys. Lett. **106A**, 312 (1984).

¹¹A shorter version of some of the elaborate discussion here was

- presented by K. S. Bedell and K. F. Quader, *Phys. Rev. B* **32**, 3296 (1985); K. F. Quader, in *Condensed Matter Theories*, edited by F. B. Malik (Plenum, New York, 1986), Vol. 1, p. 247.
- ¹²D. Pines and P. Nozières, *The Theory of Quantum Liquids* (Benjamin, New York, 1966), Vol. I.
- ¹³A. J. Leggett, *Ann. Phys.* **46**, 76 (1968); *Phys. Rev.* **140A**, 1869 (1965).
- ¹⁴D. Einzel, P. J. Hirschfeld, F. Gross, B. S. Chandrasekhar, K. Andres, H. R. Ott, J. Beurs, Z. Fisk, and J. L. Smith, *Phys. Rev. Lett.* **56**, 2513 (1986).
- ¹⁵C. Mahaux, R. Broglia, and C. Dasso, *Phys. Rep.* **120**, 1 (1985).
- ¹⁶C. M. Varma, K. Miyake, and S. Schmitt-Rink, *Phys. Rev. Lett.* **57**, 626 (1986).
- ¹⁷K. F. Quader, Proceedings of the International Conference and Symposium on Unified Concepts of Many-Body Problems, Stony Brook, New York, 1986, edited by T. T. Kuo and J. Speth (unpublished).
- ¹⁸J. Hubbard, *Proc. R. Soc. London Ser. A* **276**, 238 (1963); **281**, 401 (1964).
- ¹⁹D. D. Koelling, B. D. Dunlap, and G. W. Crabtree, *Phys. Rev. B* **31**, 4966 (1985).
- ²⁰The argument for the presence of these terms is quite general as their derivation follows from the requirement of time-reversal invariance.
- ²¹D. Vollhardt, *Rev. Mod. Phys.* **56**, 99 (1984).
- ²²W. F. Brinkman and T. M. Rice, *Phys. Rev.* **132**, 4302 (1970).
- ²³T. M. Rice and K. Ueda, *Phys. Rev. Lett.* **55**, 995 (1985).
- ²⁴P. W. Anderson and W. F. Brinkman, 1978, in *The Physics of Liquid and Solid Helium, Part II*, edited by K. H. Bennemann and J. B. Ketterson (Wiley, New York, 1978).
- ²⁵O. T. Valls and Z. Tešanović, *Phys. Rev. Lett.* **53**, 1497 (1984).
- ²⁶M. Gutzwiller, *Phys. Rev. Lett.* **10**, 159 (1963).
- ²⁷T. H. R. Skyrme, *Proc. R. Soc. London Ser. A* **260**, 1726 (1965).
- ²⁸G. E. Brown, A. D. Jackson, Mannque Rho, and V. Vento, *Phys. Lett.* **140B**, 285 (1984).
- ²⁹L. E. DeLong, R. P. Guertin, S. Hasanain, and T. Fariss, *Phys. Rev. B* **31**, 7059 (1985).
- ³⁰H. Razafimandimby, P. Fulde, and J. Keller, *Z. Phys.* **54**, 111 (1984).
- ³¹P. W. Anderson, *Phys. Rev. B* **30**, 1549 (1984).
- ³²C. J. Pethick, D. Pines, K. F. Quader, K. S. Bedell, and G. E. Brown, *Phys. Rev. Lett.* **57**, 1955 (1986).
- ³³B. Patton and A. Zaringhalam, *Phys. Lett.* **A55**, 329 (1975).
- ³⁴M. Pfizner and P. Wolffe, *Phys. Rev. B* **35**, 4699 (1987).